The Effects of External pH on Calcium Channel Currents in Bullfrog Sympathetic Neurons

Wei Zhou and Stephen W. Jones
Department of Physiology and Biophysics, Case Western Reserve University, Cleveland, Ohio 44106 USA

ABSTRACT We have investigated the effects of external pH (pH_o) on whole-cell calcium channel currents in bullfrog sympathetic neurons. The peak inward current increased at alkaline pH_o and decreased at acidic pH_o. We used tail currents to distinguish effects of pH_o on channel gating and permeation. There were large shifts in the voltage dependence of channel activation (~40 mV between pH_o 9.0 and pH_o 5.6), which could be explained by binding of H^+ to surface charge according to Gouy-Chapman theory. To examine the effects of pH_o on permeation, we measured tail currents at 0 mV, following steps to +120 mV to maximally activate the channels. Unlike most previous studies, we found only a ~10% reduction in channel conductance from pH_o 9.0 to pH_o 6.4, despite a ~25 mV shift of channel activation. At lower pH_o the channel conductance did decrease, which could be described by binding of H^+ to a site with $pK_a = 5.1$. In some cells, there was a separate slow decrease in conductance at low pH_o, possibly because of changes in internal pH. These results suggest that changes in current at $pH_o > 6.4$ result primarily from a shift in the voltage dependence of channel activation. A H^+-binding site can explain a rapid decrease in channel conductance at lower pH_o. The surface charge affecting gating has little effect on the local ion concentration near the pore, or on the channel conductance.

INTRODUCTION

Extracellular pH (pH_o) affects a variety of ionic channels, including voltage-dependent calcium channels (Ohmori and Yoshii, 1977; Begenisich and Danko, 1983; Iijima and Hagiwara, 1986; Krafte and Kass, 1988; Prod'hom et al., 1989; Tytgat et al., 1990; Klöckner and Isenberg, 1994b). Alkaline pH_o increases calcium channel currents and acidic pH_o decreases the currents. Many studies have been conducted to understand the mechanisms responsible for the modulation of calcium channels by pH_o.

Several mechanisms have been proposed for the effects of pH_o. 1) H^+ can titrate surface charges on the external face of the plasma membrane, which would change the voltage dependence of channel gating. Such voltage shifts have been observed in many cell types, and this mechanism is widely accepted. 2) The local ionic concentration near the channel pore may be affected by H^+ binding to the surface charge, possibly the same surface charge that affects channel gating (Ohmori and Yoshii, 1977; Iijima and Hagiwara, 1986). 3) H^+ can block the channel, possibly in the channel pore (Prod'hom et al., 1989; Krafte and Kass, 1988; Klöckner and Isenberg, 1994b). 4) A change in pH_o can affect intracellular pH (pH_i), which changes the channel current (Irisawa and Sato, 1986; Klöckner and Isenberg, 1994a,b). However, the relative importance of these mechanisms for the effects of pH_o has not been well defined. At least one of the reasons is that the effects of pH_o on channel gating and those on channel conductance have not been fully separated.

In the present study, we tried to determine the contributions of these mechanisms to effects of pH_o on calcium channel currents, using tail current analysis to separate effects on gating and permeation.

MATERIALS AND METHODS

Neurons were isolated from paravertebral sympathetic ganglia of adult bullfrogs (*Rana catesbeiana*) and maintained in culture at 4°C as described previously (Kuffler and Sejnowski, 1983; Jones and Marks, 1989; Zhou and Jones, 1995). The currents were recorded in the whole cell configuration (Hamill et al., 1981) using an Axopatch-200 or an Axopatch 1C patch-clamp amplifier. The standard intracellular solution consisted of (in mM) 82.6 *N*-methyl-D-glucamine chloride (NMG·Cl), 60 NMG·HEPES, 10 NMG_2·EGTA, 5 $Tris_2$·ATP, and 6 $MgCl_2$, titrated to pH 7.2 with NMG base. The standard extracellular solution contained (in mM) 117.5 NMG·Cl, 5 NMG·HEPES, 2 $BaCl_2$, and 5 of one of the following buffers: TAPS (pK_a = 8.4), 2-(*N*-morpholino)ethanesulfonic acid (pK_a = 6.1), or propionic acid (pK_a = 4.9). Where noted, 1 μM TTX was added to the extracellular solution. The series resistance of the pipettes, estimated from the amplifier settings producing optimal cancellation of the capacity transient, ranged from 0.8 to 3.0 MΩ. Series resistance compensation was at least 80%. Residual capacitative current and leakage current were digitally subtracted using scaled hyperpolarizing steps. Unless noted otherwise, currents were digitally filtered at 3 kHz after 5 kHz analog filtering and sampling at 25–62.5 kHz. The holding potential was −80 mV. All experiments were carried out at room temperature. Liquid junction potentials were less than 4 mV and were independent of pH_o, so the data are presented without correction for junction potentials.

We have previously established that calcium channel currents are well isolated under our experimental conditions, and that ~90% of the calcium channel current is carried by N-type (ω-conotoxin GVIIA-sensitive) channels (Jones and Marks, 1989; Jones and Elmslie, 1992; Zhou and Jones, 1995). In some records (e.g., Fig. 5 *A*), especially for strong depolarizations, there is a brief transient outward current, possibly a gating current, which should not affect our measurements.

pClamp (Axon Instruments, Foster City, CA) software and A-D hardware were used with IBM X86-compatible computers for the experiments

Received for publication 13 October 1995 and in final form 18 December 1995.

Address reprint requests to Dr. Stephen W. Jones, Department of Physiology and Biophysics, Case Western Reserve University, Cleveland, OH 44106. Tel.: 216-368-5527; Fax: 216-368-3952; E-mail: swj@po.cwru.edu.

© 1996 by the Biophysical Society

0006-3495/96/03/1326/09 $2.00

and analysis. Values reported are mean ± SD. Data were fitted by minimizing the sum of squared deviations, using locally written programs or the Solver function in Microsoft Excel.

When pH_o was changed between the control pH_o and acidic pH_o, the change of current had a fast phase and a slow phase (see Fig. 5 *C*). The slow phase may be caused by changes in pH_i (see Discussion). We found that for some cells 1 μM TTX in the extracellular solution could eliminate the slow component. We used only the currents from these cells in the analysis of effects of low pH_o (except Fig. 5 *C*). To separate the fast and slow effects of pH_o, we used a fast perfusion system (Jones, 1991) in all of the experiments reported in this paper. The solutions were changed by moving the electrode with the cell attached from the outlet of the tubing containing one solution to the outlet of the tubing containing another solution. When current-voltage relations were measured (Figs. 1–3), the pH_o was changed for a period of 1–2 min. For conductance measurements (Figs. 5–6), pH_o changes lasted only 10–30 s.

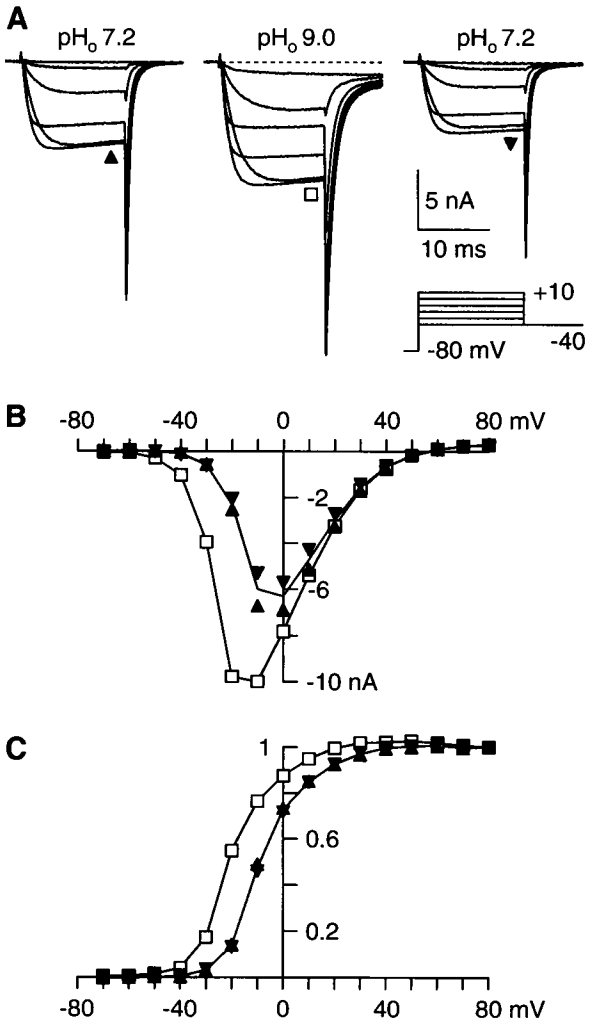

FIGURE 1 Effects of alkaline pH_o on calcium channel currents. (*A*) Currents recorded in pH_o 7.2 (*left*), pH_o 9.0 (*middle*), and after return to pH_o 7.2 (*right*). The current traces were in response to voltage pulses from −40 to +10 mV in 10-mV increments from a holding potential of −80 mV. Tail currents were recorded upon partial repolarization to −40 mV. (*B*) Current-voltage relations in pH_o 7.2 and 9.0. (*C*) Activation curves in pH_o 7.2 and 9.0, from the same cell as in *A* and *B*. No TTX was present. Activation curves were obtained from tail current measurements (Materials and Methods). The symbols used in *B* and *C* are indicated near the records in *A*. For the data in pH_o 7.2, the lines shown are the average of values recorded before and after the test pH_o.

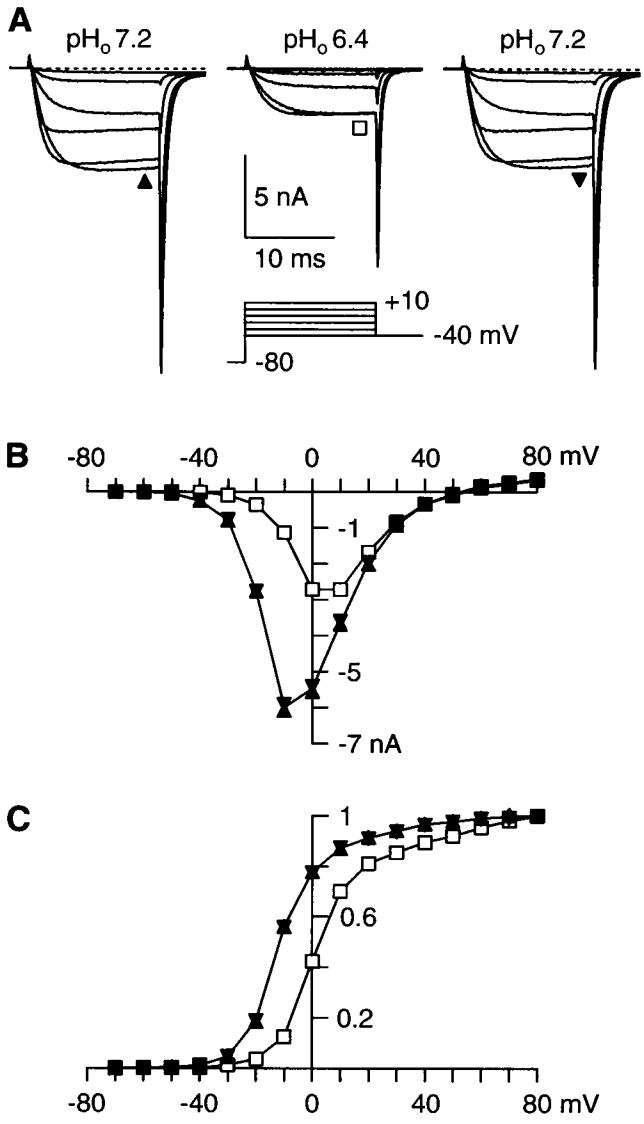

FIGURE 2 Effects of acidic pH_o on calcium channel currents. (*A*) Currents recorded in pH_o 7.2 (*left*), pH_o 6.4 (*middle*), and after return to pH_o 7.2 (*right*), shown as in Fig. 1 *A*. Tail currents were recorded at −40 mV. (*B*) Current-voltage relations in pH_o 7.2 and 6.4. (*C*) Activation curve in the solutions of pH_o 7.2 and 6.4, from the same cell as *A* and *B*. 1 μM extracellular TTX was present.

Surface potential theory

One major goal of this study was to determine the extent to which the effects of pH_o on calcium channel currents could result from binding of H^+ to surface charge. We used Gouy-Chapman theory, which assumes that there is a uniform planar distribution of charge and that ions in the bathing solution act to screen the surface charge. The limitations of Gouy-Chapman theory are well known (e.g., Hille, 1992), but in the absence of information on the actual distribution of charges on and near ion channels, it has the advantage of having a minimum of free parameters. In addition, we concluded previously that the effects of varying ionic strength and $[Ba^{2+}]_o$ can be explained by Gouy-Chapman theory, incorporating charge screening without ion binding (Zhou and Jones, 1995).

When a solution contains various ions C_i of different valences z_i, the relation between the surface potential and surface charge is given by the

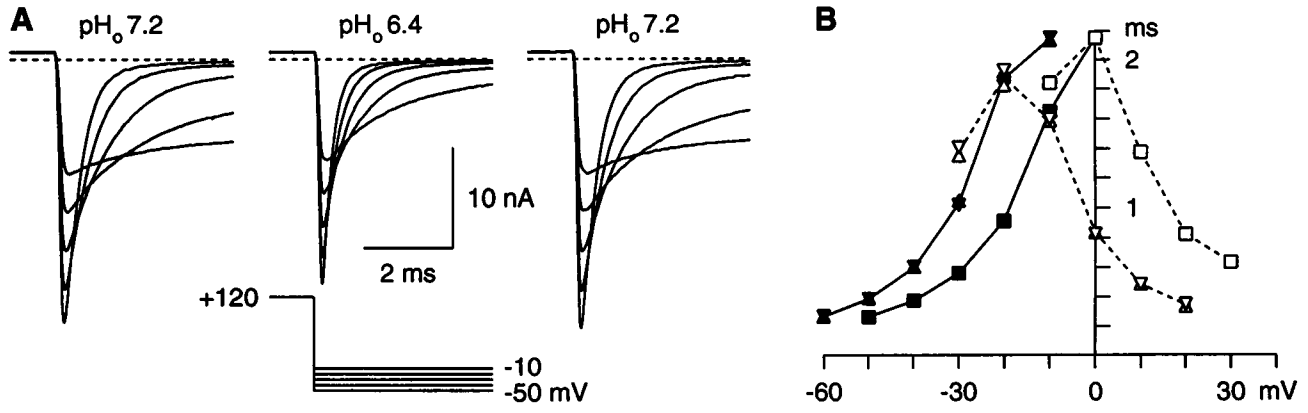

FIGURE 3 Effect of pH_o on time constants for activation and deactivation. (*A*) Sample tail currents recorded in pH_o 7.2 (*left*), pH_o 6.4 (*middle*), and after return to pH_o 7.2 (*right*). The preceding step to +120 mV was for 4 ms. Currents were digitally filtered at 4 kHz, after analog filtering at 10 kHz and sampling at 100 kHz. (*B*) Time constants for channel gating. Tail currents, from the protocol of *A*, were fitted to single exponentials starting 0.3 ms after repolarization (▲, ▼). The time course of activation, from the protocol of Figs. 1–2, was approximated by a single exponential (Jones and Marks, 1989), beginning at 0.8 ms to avoid the initial delay (△, ▽, □). Data are from the same cell as Fig. 2, in pH_o 7.2 (△), pH_o 6.4 (□, ■), and after return to pH_o 7.2 (▽).

Grahame equation (Grahame, 1947):

$$\sigma_f^2 G^2 = \sum [C_i]\{\exp(-z_i F\psi/RT)/ - 1\}, \quad (1)$$

where σ_f is the density of free surface charge (i.e., without bound H^+), ψ is the surface potential, F is the Faraday constant, R is the gas constant, T is the absolute temperature, and G is a constant equal to 270 $Å^2e^{-1}M^{1/2}$ at room temperature.

The Boltzmann equation relates the bulk ionic concentration and local ionic concentration for a given surface potential:

$$[C]_L = [C]\exp(-zF\psi/RT), \quad (2)$$

where $[C]_L$ and [C] (respectively) are the local and bulk concentrations of an ion. Specifically, for H^+, the local hydrogen ion concentration $[H^+]_L$ and local pH are related to the bulk $[H^+]$ and bulk pH by the following relations:

$$\begin{aligned}[H^+]_L &= 10^{-pH_L} = [H^+]\exp(-F\psi/RT) \\ &= 10^{-pH}\exp(-F\psi/RT).\end{aligned} \quad (3)$$

Assuming that H^+ binds to the surface charge, the relationship between free (σ_f) and total (σ) surface charge densities is

$$\sigma_f = \sigma/(1 + 10^{-pH_L}/10^{-pK_a}), \quad (4)$$

where pK_a is the dissociation constant for H^+ binding and pH_L is the local pH. If there are two different types of surface charge to which H^+ can bind, the relationship between free and total surface charge densities ($\sigma = \sigma_1 + \sigma_2$) is

$$\sigma_f = \frac{\sigma_1}{1 + 10^{-pH_L}/10^{-pK_{a1}}} + \frac{\sigma_2}{1 + 10^{-pH_L}/10^{-pK_{a2}}}. \quad (5)$$

To calculate the surface potential ψ for a given σ, pH, and solution composition, Eq. 1 and Eq. 3 were solved together with either Eq. 4 or 5, using a numerical bisection method.

Titration of surface charge by H^+ could affect permeation, in part by changing the local concentration of Ba^{2+}. From Eq. 2, the effect of a change in surface potential ($\Delta\psi$) on local $[Ba^{2+}]_o$ is

$$[Ba^{2+}]_{L,T}/[Ba^{2+}]_{L,C} = \exp(-2F\Delta\psi/RT), \quad (6)$$

where $[Ba^{2+}]_{L,T}$ and $[Ba^{2+}]_{L,C}$ are the local Ba^{2+} concentrations at test and control pH_o, respectively.

Data analysis

For the analysis of shifts in channel gating, using the voltage protocol of Figs. 1 and 2, activation curves were measured from peak tail current amplitudes at a fixed voltage (usually −40 mV), after termination of depolarization to voltages from −70 to +80 mV. The tail current amplitudes were normalized to the tail current measured after the depolarizing step to +80 mV. We found that the time to peak of the tail currents increased slightly (~50 μs) at strongly depolarized voltages. Consequently, if tail currents were measured at a fixed time after repolarization (e.g., Jones and Marks, 1989), the activation curve showed an upward "creep" at positive voltages. That effect was variable but consistently larger than when peak tail currents were used (Figs. 1 *C* and 2 *C*). The effect on the shape of the activation curve was significant, but the pH_o-induced shifts in the midpoint of the activation curve were little affected (<3 mV).

For the analysis of effects of pH_o on permeation, tail currents were measured at 0 mV after depolarization to +120 mV (Figs. 4 and 5). The initial amplitude was estimated by fitting the tail current to a single exponential and extrapolating back to the beginning of the pulse. That would tend to overestimate the amplitude, because the change in voltage is not truly instantaneous, and filtering introduces a delay. For comparision, tail amplitudes were also estimated by simply measuring the peak current, which would tend to underestimate the instantaneous current. At pH_o 7.2 or higher, tail currents at 0 mV were slow and deactivation was incomplete, and the difference between the extrapolated and peak tail current amplitudes was less than 10%. At pH_o 4.8, the difference was ~20%.

RESULTS

Effects of pH_o on current amplitude and on channel gating

Fig. 1 shows that alkaline pH_o increased the calcium channel current and moved the peak of the *I-V* curve to more negative potentials. To determine the effect of alkaline pH_o on channel gating, activation curves were obtained from the tail currents. Alkaline pH_o also moved the activation curve

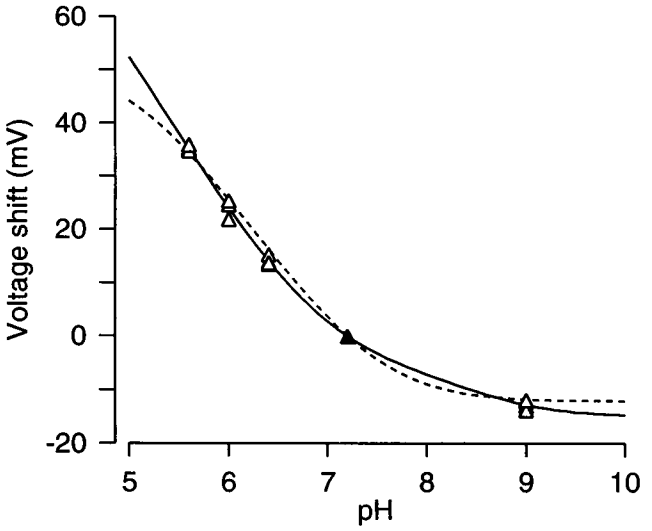

FIGURE 4 The effect of pH$_o$ on the voltage dependence of channel activation. The shift in the midpoint of the activation curve, relative to the control activation curve at pH$_o$ 7.2 (*solid symbol*), is plotted as a function of pH$_o$ (n = 3–4). The curves were fitted to the data, calculated from Gouy-Chapman theory with binding of H^+ to the surface charge (Eqs. 1–5, Materials and Methods). The dashed line is the best fit to a single type of surface charge, σ = 1 e^-/210 Å^2 with pK$_a$ = 5.9. The continuous line is the fit to two surface charges, σ_1 = 1 e^-/95 Å^2 with pK$_a$ = 5.0, and σ_2 = 1 e^-/305 Å^2 with pK$_a$ = 6.8.

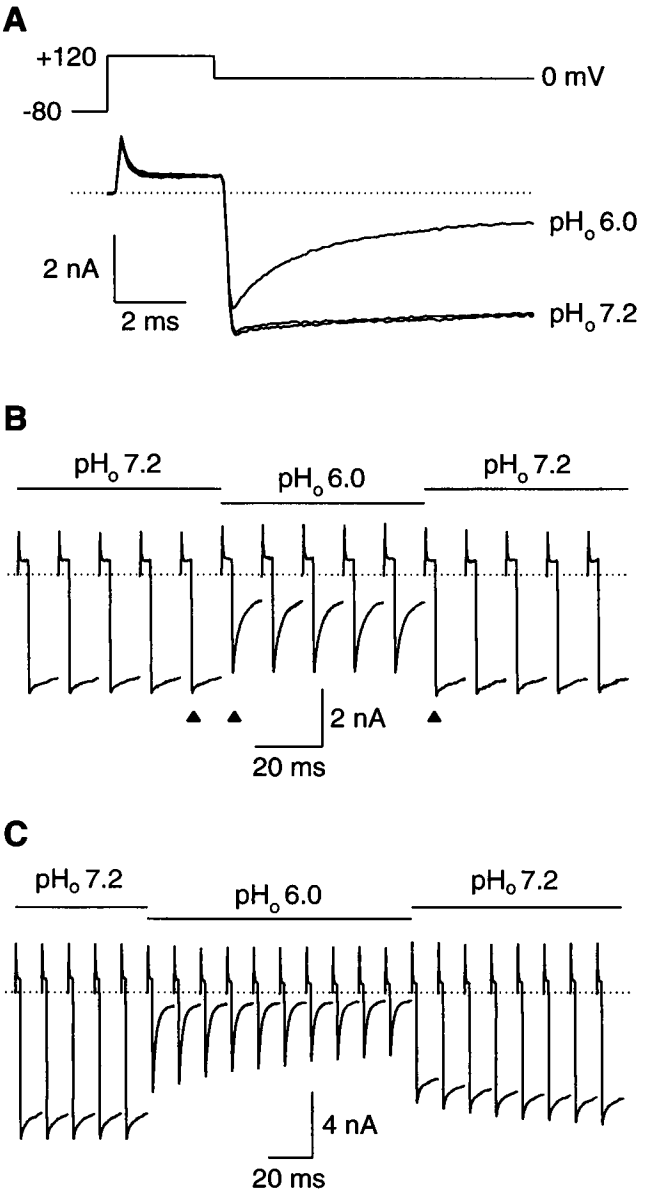

FIGURE 5 The effects of pH$_o$ on tail currents following strong depolarization. (*A*) Superimposed currents recorded in pH$_o$ 6.0 and pH$_o$ 7.2. Two current records are shown for pH 7.2, recorded before and after the current in pH$_o$ 6.0. (*B*) The time course of the pH$_o$ effect, with 1 μM extracellular TTX. Currents were recorded using the voltage protocol illustrated in *A* at 2-s intervals (the intervals between the pulses are removed for clarity). The time scale bar applies to the individual records. The pH$_o$ was changed by manually moving the cell between barrels of the flow tube system during the 2 s between voltage steps. The currents in *A* are indicated by triangles. (*C*) The time course of the pH$_o$ effect, recorded from a different cell without TTX.

in the negative direction (Fig. 1 *C*). Conversely, acidic pH$_o$ decreased the current and moved the peak of the *I-V* curve and the activation curve to more positive potentials (Fig. 2).

The shift in the activation curve was accompanied by changes in the time constants for channel activation and deactivation. At low pH$_o$, tail currents were more rapid, and activation (at positive voltages) was slower (Fig. 3). The effect could be approximated as a parallel shift along the voltage axis, but activation was shifted more than deactivation, with slightly slower kinetics near the peak of the τ-*V* curve at low pH$_o$.

The effect of pH$_o$ on the midpoint of the activation curve is shown in Fig. 4. The shifts in voltage dependence could be described reasonably well by Gouy-Chapman theory (Eq. 1–5) assuming that H^+ binds to a single, uniform surface charge density, but a slightly better fit was obtained assuming two surface charges of different density and pK$_a$. The density of free surface charge (σ_f) at pH$_o$ 7.2 was 1 e^-/291 Å^2 for a single surface charge density, and 1 e^-/111 Å^2 for two charge densities. The latter value is in much better agreement with the values we obtained previously from experiments varying $[Ba^{2+}]_o$ (1 e^-/140 Å^2) or ionic strength (1 e^-/85 Å^2) (Zhou and Jones, 1995).

Effects of pH$_o$ on channel conductance

Qualitatively, the shift in the voltage dependence of channel gating (Fig. 4) can explain the observed changes in the *I-V* curves with pH$_o$ (Figs. 1 *B* and 2 *B*). However, it is also likely that pH$_o$ affects the current through an open calcium channel. Such an effect would be expected if the channel pore sees a surface charge, or if H^+ ions block the pore. To test for effects of pH$_o$ on permeation, we used the protocol illustrated in Fig. 5 *A*. First, a 2–3-ms depolarizing pulse was given to +120 mV. Because there is little driving force on the channels at that

voltage, the cell was then partially repolarized to 0 mV, to record a tail current. The initial amplitude of that tail current depends only on the number of channels opened and the current per open channel. Assuming that the step to +120 mV produces maximum activation at all pH_o, changes in the initial tail current amplitude reflect changes in the conductance of open channels (see Discussion).

The shift in the kinetics of channel activation is reflected in the time course of the tail current (see Fig. 3). At 0 mV, in pH_o 7.2, most of the channels remain activated (Figs. 1 *B* and 2 *B*), and the relaxation rate for the channels that do close is slow (Jones and Marks, 1989). The shift of channel gating to more positive voltages in low pH_o makes 0 mV effectively a more negative voltage, so at low pH_o more channels close during the tail current, and the closing rate is more rapid (Fig. 5 *A*).

For some cells, the tail currents revealed both fast and slow changes in current upon changes between control and acidic pH_o (Fig. 5 *C*). The slow change could usually be fitted by a single exponential (τ = 5–20 s). Extrapolation of the exponential back to the time of the solution exchange, approximately the middle of the 2-s interval between test pulses, confirmed that there was an apparently instantaneous change in channel current, in addition to the slow effect. Whereas the fast change seemed to be quite consistent, the amplitude of the slow effect varied significantly from cell to cell. The slow effect appeared as a change in current amplitude, with little or no effect on gating kinetics. Slow changes in current were not observed upon changes to alkaline pH_o.

Effects of pH_o on surface charge or channel blockade by H^+ should be effectively instantaneous, at least when measured on a time scale of seconds. Therefore, we wished to analyze the fast effects of pH_o in isolation from the slow change in current. One possible explanation of a slow effect of pH_o is perturbation of pH_i (Irisawa and Sato, 1986; Klöckner and Isenberg, 1994a,b). Because we isolate calcium channel current not by blocking sodium and potassium channels, but by replacing Na^+ and K^+ with an impermeant cation (NMG^+), we considered the possibility of H^+ influx through those channels. In many but not all cells, addition of 1 μM TTX to the extracellular solution eliminated the slow effect (compare Fig. 5 *B* to 5 *C*) (see Valkina et al., 1995). In some cells, TEA partially reduced the slow effect (data not shown). Therefore, to avoid possible complications caused by changes in pH_i, we analyzed only cells where TTX could prevent the slow effect of acidic pH_o. With that precaution, rapid, reversible effects could be measured for pH_o as low as 4.8.

Fig. 6 illustrates currents for changes to pH_o 9.0, 6.4, and 5.2. Alkaline pH_o slowed channel deactivation, as expected from the effect of surface charge on the activation curve (Fig. 6 *A*). However, there was almost no effect on the initial tail current amplitude at pH_o 9.0, implying that the channel conductance is virtually unaffected. There was a detectable but small decrease in conductance at pH_o 6.4 (Fig. 6 *B*). At pH_o 5.2, channel closing was greatly accelerated, and the channel conductance was reduced by ~50%. Note that the steady-state current at 0 mV is virtually zero in pH_o 5.2 (Fig. 6 *C*, at the end of the tail current record).

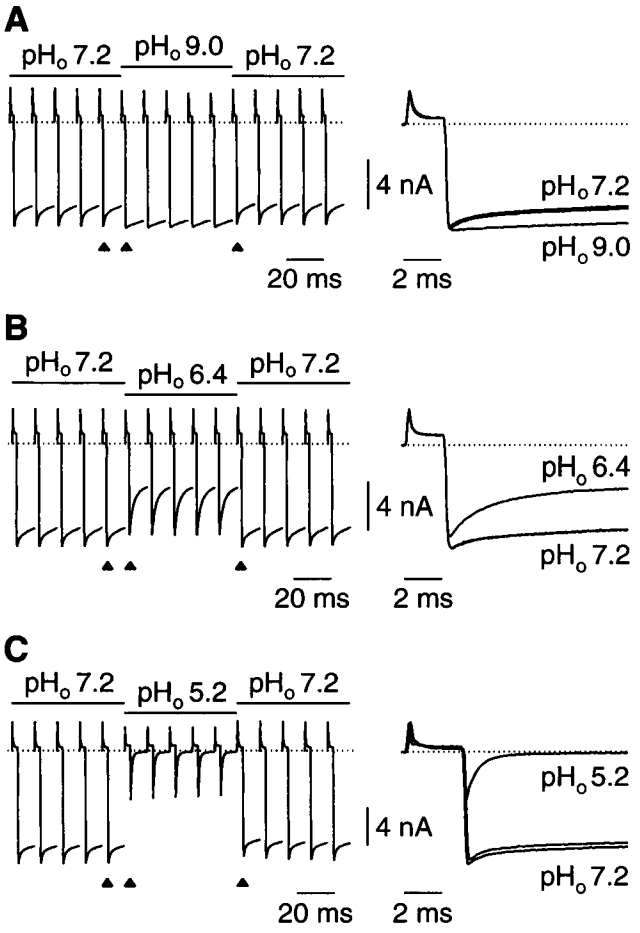

FIGURE 6 The effects of alkaline and acidic pH_o on tail currents. (*A–C*) Sample records for changes in pH_o. The time course at the left is shown as in Fig. 5, *B* and *C*, with expanded records of currents before, during, and after the change in pH_o at the right (indicated by the *triangles*). The voltage protocol was the same as in Fig. 5. Extracellular TTX (1 μM) was present for *B* and *C*.

The effect of pH_o on channel conductance is summarized in Fig. 7 *A*. The relative current amplitudes at 0 mV could be well described by the assumption that H^+ eliminates current through the channel by binding to a site with pK_a = 5.1. The simplest physical picture for such an effect is blockade of the channel pore by H^+. Other interpretations are considered in the Discussion.

For comparison, the effect of pH_o on the inward current measured at the peak of the *I-V* curve is shown in Fig. 7 *B*. The current, measured in that manner, reflects effects on both gating and permeation. Thus, the apparent pK_a, which is much less acidic, cannot be interpreted as the actual pK_a for a H^+ binding site (see Discussion).

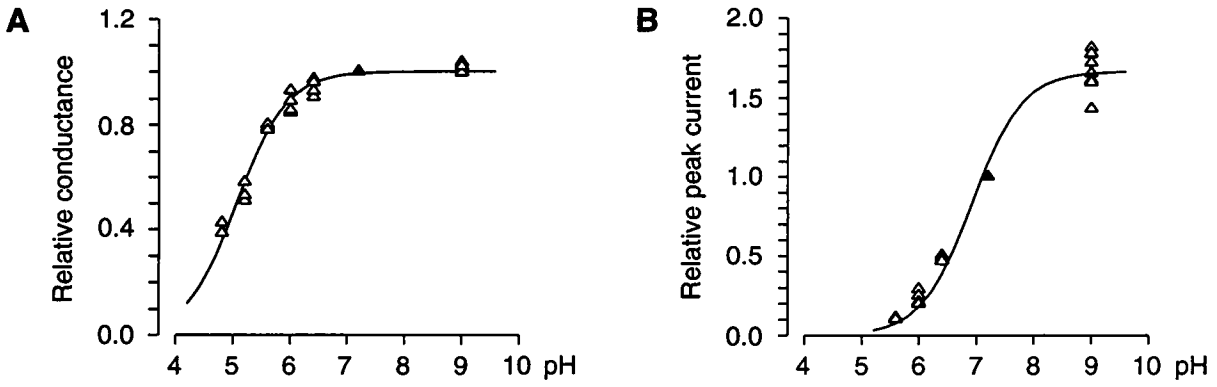

FIGURE 7 The effect of pH$_o$ on channel conductance and peak inward current. (*A*) Initial tail current amplitudes from the protocol of Figs. 4 and 5, normalized to values at pH$_o$ 7.2, as a function of pH$_o$. The amplitudes were measured from single exponential fits to the tail currents (Materials and Methods). The smooth curve is a titration curve, $1/(1 + 10^{-pH}/10^{-pK_a})$, with pK$_a$ = 5.1. The alternative measure of tail current amplitude, the peak amplitude of each tail current, gave pK$_a$ = 5.3 when plotted as a function of pH$_o$ (not shown). (*B*) The inward current at the peak of the *I-V* curve, as a function of pH$_o$. Data are from the protocol of Figs. 1 and 2. Currents are normalized to the value at pH$_o$ 7.2 (*solid*). The smooth curve is drawn for an apparent pK$_a$ = 6.92, with a maximum current 1.66 times that at pH$_o$ 7.2.

DISCUSSION

The effect of pH$_o$: gating or permeation?

For several different voltage-dependent channels, previous studies found that alkaline pH$_o$ increased the channel current and acidic pH$_o$ had the opposite effect (Hille et al., 1975; Begenisich and Danko, 1983; Yatani et al., 1984; Daumas and Andersen, 1993; Blatt, 1992). In almost all cases, changes in pH$_o$ shifted the voltage dependence of channel gating (Ohmori and Yoshii, 1977; Begenisich and Danko, 1983; Iijima and Hagiwara, 1986; Krafte and Kass, 1988; Tytgat et al., 1990; Klöckner and Isenberg, 1994; but see West et al., 1992).

Most previous studies used the peak of the *I-V* curve to evaluate the effect of pH$_o$ on channel current. We also found that the peak of the *I-V* curve changed significantly with pH$_o$, near the physiological range (Fig. 7 *B*). Also as in previous studies (e.g., Krafte and Kass, 1988; Klöckner and Isenberg, 1994b), there was almost no steady-state current when pH$_o$ was 5.0 or lower (Fig. 6 *C*). In principle, these results could reflect effects of pH$_o$ on channel gating, permeation, or both, which are mediated by binding of H^+ to surface charge or by other mechanisms such as channel block. We found that the peak tail currents decreased only ~10% from pH$_o$ 9.0 to pH$_o$ 6.4 (Figs. 5 *B* and 6 *A*), despite large changes in the *I-V* curves and activation curves in that region. We conclude that the predominant effect of pH$_o$ at pH$_o$ >6.4 is a shift in gating, with an additional reduction in channel conductance at pH$_o$ < 6.4.

Our conclusions depend on the use of whole cell tail currents to separate effects on gating and permeation. There is ample precedent for that approach, dating back to the experiments of Hodgkin and Huxley, but potential problems exist. In particular, voltage-dependent block by H^+ might affect our measurements. If block by H^+ is essentially instantaneous, as often assumed, the observed activation curve (measured from tail currents at a fixed voltage) would not be affected, and the current amplitudes at 0 mV in Figs. 5 and 6 would reflect the steady-state block level, so our conclusions would be unaffected. If H^+ block were resolved by the clamp, the conductance measurements (Figs. 5–8) would reflect the steady-state block of the channel at +120 mV (or if the block is only partially resolved, a block intermediate between the steady-state values at 0 mV and +120 mV).

We did observe a subtle change in the shape of the activation curve in most cells (see Figs. 1 *C* and 2 *C*), a slight upward "creep" at strongly depolarized voltages, which was more prominent at low pH$_o$. This raises the interesting possibility that the shape of the activation curve, which deviates from a simple Boltzmann relation at normal pH$_o$ (Bean, 1989), might reflect a voltage-dependent effect of pH$_o$ on the channel. That will require further study.

We can rule out an extreme interpretation, that the shift in the activation curve results entirely from H^+ block, with stronger block at more negative voltages. Simulations of such an effect (not shown) do not produce a parallel shift along the voltage axis over a wide pH$_o$ range (>1 pH unit), but decrease the slope of the activation curve at low pH$_o$ (essentially, the effective valence of H^+ block would subtract from the normal valence for gating). Experimentally, pH$_o$ has little effect on the steepness of the activation curve in the middle of the voltage range (Figs. 1 *C* and 2 *C*), and the "creep" at positive voltages should have little impact on the midpoint of the activation curve (our measure of shifts in gating). The effects of pH$_o$ on activation kinetics, with faster channel closing but slower opening at low pH$_o$ (Fig. 3), support the interpretation that the primary effect of pH$_o$ (above pH$_o$ 6.4) is a shift of activation kinetics along the voltage axis. The small deviations from a purely parallel shift, observed both for the activation curves and for the τ-*V*

curves, may reflect a voltage-dependent block by H^+, but other interpretations are possible.

Alternatively, if the "creep" in the activation curves at low pH_o results from an effect on gating, depolarizations to +120 mV might not produce full channel activation at low pH_o. If so, the effect of pH_o on channel conductance reported here would actually be an overestimate.

In principle, single-channel recording could separate effects on gating and permeation more directly. However, the rapid gating of N-type calcium channels would be a problem, as would channel rundown in outside-out patches (which would be necessary for direct comparision of channel amplitudes at different pH_o). In addition, the high $[Ba^{2+}]_o$ normally used for recording single calcium channels would strongly screen surface charges, and competition between Ba^{2+} and H^+ could reduce the potency of H^+ block (Prod'hom et al., 1989). Although it is possible to record macroscopic currents carried by monovalent cations through N-type channels, at the single-channel level it would be difficult to distinguish such channels from the many other ion channels found in sympathetic neurons.

Despite the considerations discussed above, we can conclude that pH_o has little effect on channel conductance above pH_o 6.4 and that the effect of pH_o on the *I-V* curve reflects the ~25 mV shift in the activation curve from pH_o 9.0 to pH_o 6.4 (Fig. 4). That interpretation is supported by the observation that the *I-V* curves are affected little at voltages well above the point of peak inward current (Figs. 1 *B* and 2 *B*), because at those positive voltages the channels are almost fully opened. Krafte and Kass (1988) reached a similar conclusion for cardiac calcium channels, using fits to a Boltzmann relation assuming a linear open-channel *I-V* as a semiquantitative separation of gating and permeation, although they found that the increase in current at alkaline pH_o could not be entirely explained by shifts in gating.

Why does measuring the peaks of the *I-V* curves at different pH_o give such a different answer from measuring changes in channel conductance (Fig. 7)? The channel open probabilities at the voltage producing peak inward current might be very similar, because the expected shifts along the voltage axis for the activation curve and the peak of *I-V* curve are almost the same (Zhou and Jones, 1995). However, the electrical driving force across the channel would be very different, especially if there is little surface charge associated with permeation.

Taken alone, our data on pH_o are consistent with either one or two populations of surface charge (Fig. 4). However, the net surface charge density at pH_o 7.2 is in much better agreement with our previous results if two surface charge densities are assumed. Multiple populations of surface charge with different pK_a for H^+ binding have been proposed previously by Hille et al. (1975) for Na^+ channels and by Kwan and Krafte (1993) for calcium channel gating in cardiac ventricular cells.

Changes in pH_o may change pH_i

A change in pH_o can affect pH_i (Austin and Wray, 1993; Klöckner and Isenberg, 1994a,b). However, we were surprised to see evidence for such an effect even with 60 mM HEPES as the intracellular pH buffer. Certainly, other interpretations of the slow effect of low pH_o (Fig. 5 *C*) are possible. However, the slow effect was significantly reduced when the intracellular pH buffer was set at 6.8 instead of 7.2 (data not shown), consistent with a reduction in the effect of H^+ influx. Changes in pH_i between 7 and 6 can produce substantial decreases in calcium channel current (Irisawa and Sato, 1986).

As the goal of this study was to understand the fast effects of pH_o, we have concentrated on isolating that effect from the slow changes in current, rather than characterizing the slow effect in any detail. It is important to note that mechanistic interpretation of the effects of pH_o required distinguishing the fast and slow effects. It is possible that slow effects of low pH_o contributed to the absence of detectable current near pH_o 5 in some previous studies. Indeed, Klöckner and Isenberg (1994b) found almost no whole cell calcium current when pH_o was 5.0 (despite clearly detectable single-channel currents), which they attributed to effects of pH_o on pH_i. Our ability to measure channel conductance at pH_o as low as 4.8 (Fig. 7 *A*) depended on separation of the fast and slow effects of pH_o, as well as the use of tail currents after strong depolarizations to overcome the strong shift of activation kinetics at low pH_o.

Effect of acidic pH_o on channel conductance: block, or surface charge?

Fig. 7 *A* demonstrates that the reduction in channel conductance at strongly acidic pH_o ($pH_o \leq 6.4$) can be explained by a titrable weak acid site with $pK_a = 5.1$. One possibility is blockade of the channel pore by H^+. Effects of H^+ on single L-type calcium channels have been interpreted as allosteric (Pietrobon et al., 1989; Prod'hom et al., 1989), but Root and MacKinnon (1994) have argued that true pore block is more likely, since the observed deviations from bimolecular kinetics could be explained by proton transfer from buffer molecules. The fit in Fig. 7 *A* assumes that binding of a single proton produces full channel block, but we cannot rule out a reduction in channel conductance and/or multiple H^+ sites.

However, there is an alternative interpretation, that binding of H^+ to surface charge reduces the channel conductance by reducing the local concentration of Ba^{2+} ($[Ba^{2+}]_L$). Therefore, we used Gouy-Chapman theory (Eqs. 1–6) to calculate the expected effect of pH_o on channel conductance.

Several steps are involved in this calculation. First, for given surface charge densities and pK_a values (chosen as described below), Eqs. 1–5 were used to calculate the surface potential (ψ) as a function of pH_o. Next, Eq. 6 was used to calculate the change in $[Ba^{2+}]_L$, relative to the value at

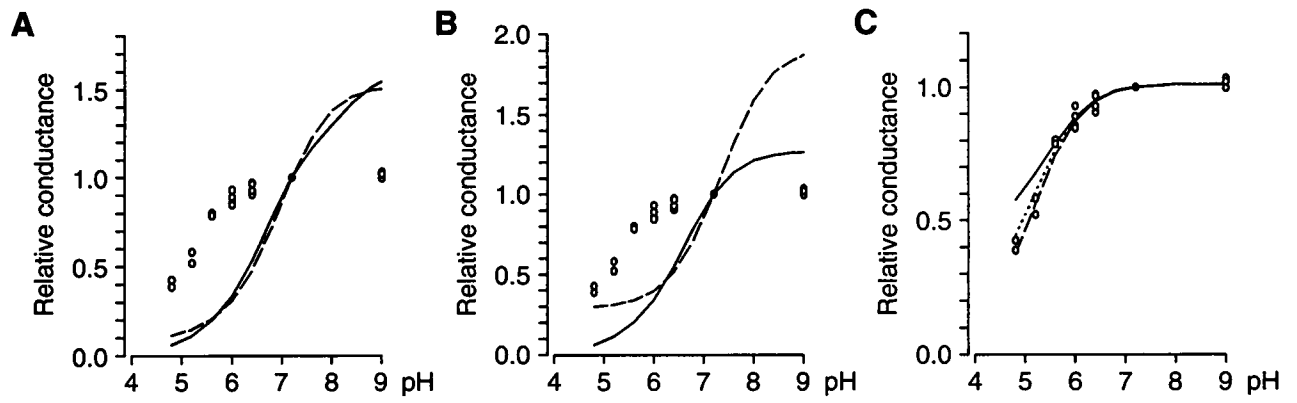

FIGURE 8 Can the effect of pH$_o$ on channel conductance be explained by surface charge? The data points are the relative tail current amplitudes at 0 mV and are the same as those shown in Fig. 7 *A*. (*A*) The effect expected if the channel pore sees the same surface charge as the voltage sensor. Two possibilities were considered (see Fig. 4): a single type of surface charge of σ = 1 e$^-$/210 Å^2 with pK$_a$ = 5.9 (– – –); two types of surface charge, σ_1 = 1 e$^-$/95 Å^2 with pK$_a$ = 5.0 and σ_2 = 1 e$^-$/305 Å^2 with pK$_a$ = 6.8 (——). (*B*) The effect expected if the channel pore sees only one of two types of surface charge seen by the voltage sensor. ——, σ_1 = 1 e$^-$/95 Å^2 with pK$_a$ = 5.0; – – –, σ_2 = 1 e$^-$/305 Å^2 with pK$_a$ = 6.8. (*C*) The effect expected if the channel pore sees a surface charge that is totally different from that seen by the voltage sensor. Three assumed charge densities are shown, σ = 1 e$^-$/100 Å^2 with pK$_a$ = 3.5 (– – –), 1 e$^-$/400 Å^2 with pK$_a$ = 4.4 (·····), and 1 e$^-$/1000 Å^2 with pK$_a$ = 5.1 (——). For each σ, the pK$_a$ was varied to produce the best fit.

the control pH$_o$ of 7.2. In addition to the change in $[Ba^{2+}]_L$, a surface potential will also affect the energy profile experienced by an ion permeating the pore. That is, the transchannel voltage will not be the macroscopic membrane potential V_M, but $V_M - \psi$ (MacKinnon et al., 1989; Zhou and Jones, 1995). Because of the voltage shift, simple comparison of the currents measured at V_M = 0 mV would not be valid, as the effective driving force changes with pH$_o$. To account for this, we used the instantaneous *I-V* relation for the fully activated channel, measured at pH$_o$ 7.2 (Zhou and Jones, 1995). As an example, for a 15-mV depolarizing shift caused by acidic pH$_o$ ($\Delta\psi$ = +15 mV), $[Ba^{2+}]_L$ would decrease to 0.306 of the value at pH$_o$ 7.2 (Eq. 6). But the current at 0 mV in the acidic pH$_o$ should be compared to the current at −15 mV in pH$_o$ 7.2, which was 1.67-fold larger than at 0 mV (by interpolation of the instantaneous *I-V*). Therefore, the net predicted effect is that the current in the acidic pH$_o$ would be 0.511 of the value at pH$_o$ 7.2 (0.306 × 1.67). Thus, the voltage shift will tend to cancel the effect of the decreased $[Ba^{2+}]_L$, but the cancellation is not complete.

To begin with, we assumed that the same surface charge is seen by the pore and the voltage sensor. Whether one or two surface charge densities were assumed (see Fig. 4), the predicted effect on channel conductance was far larger than observed (Fig. 8 *A*). In particular, a substantial increase in conductance was predicted for changes in alkaline pH$_o$, which was not observed experimentally (Figs. 6 *A* and 7 *A*). It is conceivable that the pore might see only one of two surface charge densities seen by the voltage sensor, but that also predicts changes in conductance around pH$_o$ 7.2 that are much larger than observed (Fig. 8 *B*). These calculations suggest that the channel pore and the voltage sensor do not see the same surface charge. However, it is possible that the same physical surface charge affects both gating and permeation, but that the pore is electrically farther from the surface charge. In that case (which is not considered in Gouy-Chapman theory), we could still conclude that the pore and voltage sensor do not see the same surface potential.

Several groups have suggested that the channel pore might see the same surface potential that affects the channel gating (Ohmori and Yoshii, 1977; Iijima and Hagiwara, 1986). Our results strongly support the opposite conclusion, which we (Zhou and Jones, 1995) and others (e.g., Begenisich, 1975; Wilson et al., 1983) have drawn previously on other grounds.

Perhaps the pore experiences a surface charge, but one that is distinct from that near the voltage sensor. The experimental data could be described well by Gouy-Chapman theory with relatively high densities of surface charge, but if σ at the pore is less than 1 e$^-$/600 Å^2, the change in $[Ba^{2+}]_L$ was too small to account for the observed decrease in channel conductance at low pH$_o$ (Fig. 8 *C*).

From the present data, we cannot exclude the possibility that pH affects channel conductance by binding to surface charge, but the charge density required is inconsistent with our previous results (Zhou and Jones, 1995). Our experiments varying $[Ba^{2+}]_o$ and ionic strength found that σ near the channel pore was 1 e$^-$/1500 Å^2 or less at pH$_o$ 7.2. For charge densities in the range 1 e$^-$/100 Å^2 to 1 e$^-$/500 Å^2, with pK$_a$ values of 3.5–4.5 (Fig. 8 *C*), little surface charge would bind H$^+$ at pH$_o$ 7.2, and we would have seen much higher charge densities associated with permeation in our previous experiments. Conversely, a surface charge that is 1 e$^-$/1500 Å^2 or less at pH$_o$ 7.2 could account for only a small portion of the effect reported here of low pH$_o$ on channel conductance. We suggest that H$^+$ block or titration of some site, possibly in the channel pore, is primarily responsible for the alteration of the channel conductance at pH$_o$ < 6.4.

Supported in part by National Institutes of Health grant NS 24471 to SWJ, who is an Established Investigator of the American Heart Association.

REFERENCES

Austin, C., and S. Wray. 1993. Extracellular pH signals affect rat vascular tone by rapid transduction into intracellular pH changes. *J. Physiol. (Lond.).* 466:1–8.

Bean, B. P. 1989. Neurotransmitter inhibition of neuronal calcium currents by changes in channel voltage dependence. *Nature.* 340:153–156.

Begenisich, T. 1975. Magnitude and location of surface charges in *Myxicola* giant axon. *J. Gen. Physiol.* 66:47–65.

Begenisich, T., and M. Danko. 1983. Hydrogen ion block of the sodium pore in squid giant axons. *J. Gen. Physiol.* 82:599–618.

Blatt, M. R. 1992. K^+ channels of stomatal guard cells. Characteristics of the inward rectifier and its control by pH. *J. Gen. Physiol.* 99:615–644.

Daumas, P., and O. S. Andersen. 1993. Proton block of rat brain sodium channels. Evidence for two proton binding sites and multiple occupancy. *J. Gen. Physiol.* 101:27–43.

Grahame, D. C. 1947. The electrical double layer and the theory of electrocapillarity. *Chem. Rev.* 41:441–501.

Hamill, O. P., A. Marty, E. Neher, B. Sakmann, and F. J. Sigworth. 1981. Improved patch-clamp techniques for high-resolution current recording from cells and cell-free membrane patches. *Pflügers Arch.* 391:85–100.

Hille, B. 1992. Ionic Channels of Excitable Membranes. Sinauer Associates, Sunderland, MA.

Hille, B., A. M. Woodhull, and B. I. Shapiro. 1975. Negative surface charge near sodium channels of nerve: divalent ions, monovalent ions, and pH. *Phil. Trans. R. Soc. Lond.* B270:301–318.

Iijima, T., and S. Hagiwara. 1986. Effects of the external pH on Ca channels: experimental and theoretical considerations using a two-site, two-ion model. *Proc. Natl. Acad. Sci. USA.* 83:654–658.

Irisawa, H., and R. Sato. 1986. Intra- and extracellular actions of protons on the calcium current of isolated guinea pig ventricular cells. *Circ. Res.* 59:348–355.

Jones, S. W. 1991. Time course of receptor-channel coupling in frog sympathetic neurons. *Biophys. J.* 60:502–507.

Jones, S. W., and K. S. Elmslie. 1992. Separation and modulation of calcium currents in bull-frog sympathetic neurons. *Can. J. Physiol. Pharmacol.* 70:S56–S63.

Jones, S. W., and T. N. Marks. 1989. Calcium currents in bullfrog sympathetic neurons. I. Activation kinetics and pharmacology. *J. Gen. Physiol.* 94:151–167.

Klöckner, U., and G. Isenberg. 1994a. Intracellular pH modulates the availability of vascular L-type Ca^{2+} channels. *J. Gen. Physiol.* 103:647–663.

Klöckner, U., and G. Isenberg. 1994b. Calcium channel current of vascular smooth muscle cells: extracellular protons modulate gating and single channel conductance. *J. Gen. Physiol.* 103:665–678.

Krafte, D. S., and R. S. Kass. 1988. Hydrogen ion modulation of Ca channel current in cardiac ventricular cells. Evidence for multiple mechanisms. *J. Gen. Physiol.* 91:641–657.

Kuffler, S. W., and T. J. Sejnowski. 1983. Peptidergic and muscarinic excitation at amphibian sympathetic synapses. *J. Physiol. (Lond.).* 341:257–278.

Kwan, Y. W., and R. S. Kass. 1993. Interactions between H^+ and Ca^{2+} near cardiac L-type calcium channels: evidence for independent channel-associated binding sites. *Biophys. J.* 65:1188–1195.

MacKinnon, R., R. Latorre, and C. Miller. 1989. Role of surface electrostatics in the operation of a high-conductance Ca^{2+}-activated K^+ channel. *Biochemistry.* 28:8092–8099.

Ohmori, H., and M. Yoshii. 1977. Surface potential reflected in both gating and permeation mechanisms of sodium and calcium channels of the tunicate egg cell membrane. *J. Physiol. (Lond.).* 267:429–463.

Pietrobon, D., B. Prod'hom, and P. Hess. 1989. Interactions of protons with single open L-type calcium channels. pH dependence of proton-induced current fluctuations with Cs^+, K^+, and Na^+ as permeant ions. *J. Gen. Physiol.* 94:1–21.

Prod'hom, B., D. Pietrobon, and P. Hess. 1989. Interactions of protons with single open L-type calcium channels. Location of protonation site and dependence of proton-induced current fluctuations on concentration and species of permeant ion. *J. Gen. Physiol.* 94:23–42.

Root, M. J., and R. MacKinnon. 1994. Two identical noninteracting sites in an ion channel revealed by proton transfer. *Science.* 265:1852–1856.

Tytgat, J., B. Nilius, and E. Carmeliet. 1990. Modulation of the T-type cardiac Ca channel by changes in proton concentration. *J. Gen. Physiol.* 96:973–990.

Valkina, O. N., O. V. Vergun, V. B. Turovetsky, and B. I. Khodorov. 1995. Changes of cytoplasmic pH in frog nerve fibers during K^+-induced membrane depolarization. *FEBS Lett.* 361:145–148.

West, G. A., D. C. Leppla, and J. M. Simard. 1992. Effects of external pH on ionic currents in smooth muscle cells from the basilar artery of the guinea pig. *Circ. Res.* 71:201–209.

Wilson, D. L., K. Morimoto, Y. Tsuda, and A. M. Brown. 1983. Interaction between calcium ions and surface charge as it relates to calcium currents. *J. Membr. Biol.* 72:117–130.

Yatani, A., A. M. Brown, and A. Akaike. 1984. Effect of extracellular pH on sodium current in isolated single rat ventricular cells. *J. Membr. Biol.* 78:163–168.

Zhou, W., and S. W. Jones. 1995. Surface charge and calcium channel saturation in bullfrog sympathetic neurons. *J. Gen. Physiol.* 105: 441–462.